




Approximate helical symmetry in compact binaries

Aniket Khairnar ^{1,*} Leo C. Stein ¹ and Michael Boyle ²

¹*Department of Physics and Astronomy, University of Mississippi, University, MS 38677, USA*

²*Cornell Center for Astrophysics and Planetary Science,
Cornell University, Ithaca, New York 14853, USA*

The inspiral of a circular, non-precessing binary exhibits an approximate helical symmetry. The effects of eccentricity, precession, and radiation reaction break the exact symmetry. We estimate the failure of this symmetry using the flux of the BMS charge corresponding to helical symmetry carried away by gravitational waves. We analytically compute the helical flux for binaries moving on eccentric orbits and quasi-circular orbits without precession using post-Newtonian theory. The helical flux is non-vanishing at the 0PN order for eccentric orbits as expected. We analytically predict the helical flux to be at a relative 5PN order for quasi-circular non-precessing binaries. This prediction is compared with 113 quasi-circular non-precessing numerical relativity waveforms from the SXS catalog. We find good agreement between analytical and numerical results for quasi-circular non-precessing binaries establishing that helical symmetry starts to break at 5PN for these binaries.

I. INTRODUCTION

Einstein’s field equations of general relativity have a non-linear structure. This leads to significant difficulties in solving them analytically for arbitrary gravitational sources. Approximate analytical techniques like post-Newtonian (PN) theory and black hole perturbation theory (BHPT) are used to solve them for the cases of either weak fields and slow motions, or a sufficiently small perturbation to a black hole spacetime. But these methods are invalid close to the merger of a black hole binary, when GR is highly dynamical and non-linear. Only numerical relativity (NR) can solve Einstein’s equations in this strong field regime. However since NR is expensive, we try to exploit analytical results whenever possible, and using symmetries—even approximate symmetries—is indispensable. In this work, we quantify an under-appreciated approximate symmetry exhibited by compact binary systems.

When a compact binary has a closed circular orbit with no precession, then the spacetime exhibits an exact helical Killing vector. This concept of helical symmetry has been used to impose quasi-stationarity in the initial data of binary black holes [1, 2], and to study orbital dynamics in PN theory [3–8]. In recent works, this symmetry has been used to establish laws of binary black hole mechanics for non-spinning [9] and spinning particles [10] in studies of the gravitational self-force. However in a real inspiralling binary, the helical symmetry is only approximate, restricting its applicability.

For an inspiralling quasi-circular binary, or one with a precessing orbital plane, or one with eccentric orbits, this symmetry is broken. The effects of eccentricity, precession, and radiation reaction break the symmetry in decreasing order of importance. We say such spacetimes exhibit an approximate helical symmetry based on the timescales over which these effects operate. The eccen-

tricity is certainly the dominant effect because it operates on an orbital timescale, completely breaking the symmetry. Precession of the orbital plane operates on timescale longer than the orbital timescale, while radiation reaction operates on the longest. Therefore radiation reaction is the weakest effect to break the helical symmetry.

We want to analytically compute the effect of approximate symmetry breaking using PN theory. However we are limited by today’s PN results not going to sufficiently high order. Thus we quantify the approximate helical symmetry by comparing it with the SXS catalog of NR simulations [11], supporting our analytical understanding. We use the initial orbital parameters of the binary system, like eccentricity and dimensionless spin vectors, to sort the simulations into categories of eccentric non-precessing, quasi-circular precessing, and quasi-circular non-precessing systems. In this way, we isolate the various effects that break the helical symmetry.

Specifically, to quantify the symmetry, we will apply Noether’s theorem [12] to compact binaries’ gravitational waves, which encode the approximate helical symmetry. From Noether’s theorem, the charge corresponding to a continuous symmetry would be conserved, whereas a broken symmetry implies a non-vanishing flux of the associated charge at future null infinity, \mathcal{I}^+ . Thus gravitational waves carry away a flux of the helical charge. The behavior of the helical flux helps us to establish its dependence on the source parameters like mass ratio, frequency, and eccentricity. Our analysis underscores that one cannot always ignore the breaking of the helical symmetry. As suggested by [13], this implies that quasi-circular orbits remain quasi-circular under radiation reaction, to a very high PN order.

We begin with Section II by introducing the concept of helical symmetry and the corresponding helical flux mathematically. We present the non-vanishing helical fluxes for the three effects appearing at different PN orders. Then we provide analytical results for the effect of eccentricity and radiation reaction on breaking the symmetry in Section III. We find the analytical result of helical flux for an eccentric non-precessing binary to

* akhairna@go.olemiss.edu

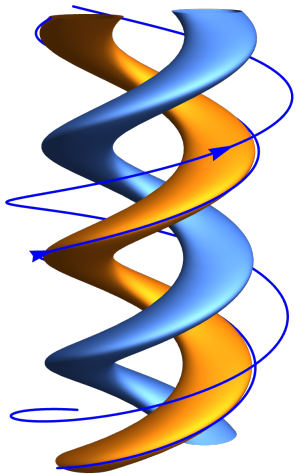


FIG. 1. Schematic representation of a binary black hole spacetime with a helical symmetry.

be at a relative 0PN to energy flux. Then we proceed to the analytical computation of helical flux for a quasi-circular non-precessing binary that is relatively complex. We find it to be at a relative 5PN order to the energy flux that matches with our numerical results presented in Section IV. In Section V, we conclude with our discussion on the choice of angular velocity in numerical analysis, the modulations observed in the helical flux, and the prospects of our work in the future.

II. HELICAL SYMMETRY

Helically symmetric spacetimes have a global symmetry generated by a helical Killing vector field. Mathematically it can be represented as a combination of time translation and rotation as

$$K^\alpha \partial_\alpha = \partial_t + \Omega \partial_\phi, \quad (1)$$

where ∂_t is the generator of time translations and ∂_ϕ is the generator of rotation about a symmetry axis; in an asymptotic region, we can say the rotation is about a vector \hat{L} . Here Ω is the asymptotic frequency of the rotation measured by observers at future null infinity. For this symmetry to be exact, Ω must simply be a constant. A spacetime exhibiting this symmetry is represented in Fig. 1.

Our systems of interest are slowly-evolving compact binaries, inspiralling due to radiation reaction. Here Ω is approximately half the frequency of the dominant (2, 2) mode radiation (and is related to the orbital frequency of the binary measured by local observers as shown in [5]).

The effects of eccentricity, precession, and radiation reaction break the exact symmetry to only an approximate symmetry, which we want to quantify. As per Noether's theorem, the charge corresponding to a global symmetry would be conserved. Therefore the flux of this charge would be identically zero for an unbroken symmetry.

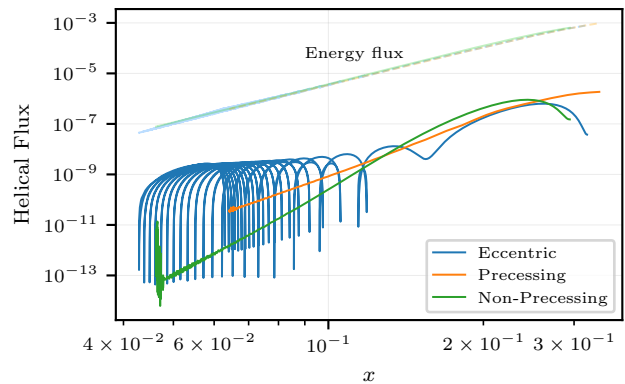


FIG. 2. Helical flux computed from an eccentric (green, SXS:BBH:2599, $e = 0.21$), precessing (orange, SXS:BBH:2450, $\chi_{1,2}^\perp \approx 0.5$) and non-precessing quasi-circular (blue, SXS:BBH:3912) SXS simulation. These fluxes are plotted as a function of the post-Newtonian parameter x , Eq. (10). For reference, the energy fluxes for the three systems are plotted (same colors but dashed) on the same axes.

For asymptotically flat spacetimes, the asymptotic symmetry group at \mathcal{I}^+ is not the Poincaré group, but an enlarged group called the Bondi–van der Burg–Metzner–Sachs (BMS) group [14–16]. If Ω were simply constant, then $K^\alpha \partial_\alpha$ would be a BMS generator. The flux at \mathcal{I}^+ due to a BMS vector field ξ is [17]

$$F_\xi = -\frac{1}{32\pi} \int d^2x N^{ij} \mathcal{L}_\xi C_{ij}, \quad (2)$$

where C_{ij} is the Bondi news aspect and N_{ij} is the Bondi news. The helical vector field can be expressed in Bondi coordinates as

$$\xi = K^\alpha \partial_\alpha = \partial_u + (\vec{\Omega} \times \vec{x}) \cdot \vec{\partial}. \quad (3)$$

Using the linearity of Lie derivatives it can be shown that

$$F_\xi = \dot{E} - \Omega \cdot \dot{\mathbf{L}}, \quad (4)$$

where \dot{E} is energy flux, $\dot{\mathbf{L}}$ is angular momentum flux, and ξ is the helical vector field as defined in Eq. (3).

A real binary has a time-dependent frequency, so we promote Ω to $\Omega(u)$, and will quantify the failure of satisfying the exact symmetry by computing

$$F_\xi = \dot{E} - \Omega(u) \cdot \dot{\mathbf{L}}. \quad (5)$$

Eccentricity, precession, and radiation reaction will all produce non-vanishing helical fluxes at \mathcal{I}^+ at different PN orders. Figure 2 demonstrates the lack of cancellation in an eccentric system (blue), followed by cancellations at higher PN orders in a precessing system (orange) and finally a non-precessing quasi-circular system (green).

III. ANALYTICAL RESULTS

Let us analytically compute the helical flux for eccentric binary systems and quasi-circular, non-precessing

systems. The inspiral of a binary evolves gradually due to the emission of gravitational radiation. We employ the post-Newtonian multipolar post-Minkowskian (PN-MPM) formalism as discussed in [5] to study such slow-moving and weak field sources.

A. Eccentricity

The helical symmetry is intuitively absent in eccentric binaries to leading order in perturbation theory. A leading order PN-MPM computation of the helical flux would suffice to obtain the non-vanishing helical flux. We follow the approach outlined in [5, 18] using the quasi-Keplerian parametrization of the motion of the binary. We review the steps necessary to get the helical flux for an eccentric binary.

The binary system is described in the following way. We have two bodies with masses m_1 and m_2 moving on an elliptical orbit with eccentricity e and semimajor axis a . In the reduced one-body description, a body of reduced mass $\mu = m_1 m_2 / (m_1 + m_2)$ is orbiting around a central body of mass $m = m_1 + m_2$, that is situated at one of the foci of the ellipse. We primarily use the symmetric mass ratio $\nu = \mu/m$ instead of μ . The motion is planar and perpendicular to the direction of orbital angular momentum L . The orbital separation is $r = |\mathbf{r}|$ and the relative velocity is \mathbf{v} . The radius r and orbital phase or true anomaly ϕ can be expressed in terms of the eccentric anomaly u as

$$r = a(1 - e \cos u) + \mathcal{O}\left(\frac{1}{c^8}\right), \quad (6)$$

$$\phi - \phi_p = 2K \arctan \left[\left(\frac{1+e}{1-e} \right)^{1/2} \tan \frac{u}{2} \right] + \mathcal{O}\left(\frac{1}{c^4}\right), \quad (7)$$

where ϕ_p is the phase at the pericenter, and K is the precession of the pericenter per orbit. The eccentric anomaly is related to the mean anomaly l by Kepler's equation, which to leading order is

$$l = n(t - t_p) = u - e \sin u + \mathcal{O}\left(\frac{1}{c^4}\right), \quad (8)$$

where n is the mean motion, and t_p is the time of pericenter passage. These orbital elements can be expressed

in terms of the dimensionless energy ε and dimensionless angular momentum j , defined in terms of the energy E and specific angular momentum $h = J/Gm$ as

$$\varepsilon = -\frac{2E}{\mu c^2}, \quad j = -\frac{2Eh^2}{\mu^3}. \quad (9)$$

The expansion parameter x in PN theory for eccentric binaries is related to the orbital frequency Ω and the dimensionless parameters as

$$x = \left(\frac{G m \Omega}{c^3} \right)^{2/3}, \quad (10a)$$

$$x = \varepsilon \left\{ 1 + \varepsilon \left[-\frac{5}{4} + \frac{1}{12}\nu + \frac{2}{j} \right] + \mathcal{O}(\varepsilon^2) \right\}. \quad (10b)$$

The orbital elements defined earlier can be expanded in terms of x using intermediate relations with ε given in [5]

$$a = \frac{Gm}{xc^2} \left\{ 1 + \mathcal{O}\left(\frac{1}{c^2}\right) \right\}, \quad (11a)$$

$$n = \frac{x^{3/2} c^3}{Gm} \left\{ 1 + \mathcal{O}\left(\frac{1}{c^2}\right) \right\}, \quad (11b)$$

$$K = 1 + \mathcal{O}\left(\frac{1}{c^2}\right). \quad (11c)$$

The contribution from the source quadrupole moment will be sufficient to obtain the helical flux to the leading order. The quadrupole moment at Newtonian order is given by

$$\mathbf{I}_{ij} = \nu m x_{\langle i} x_{j \rangle}. \quad (12)$$

It is straightforward to compute the helical flux using Eq. (5), computing energy and angular momentum flux following [5]. We provide the instantaneous results for the fluxes instead of orbit averaged expressions,

$$\dot{E} = \frac{32c^5 \nu^2 x^5}{5G(1 - e \cos u)^6} \left(1 - \frac{1}{24}e^2 \cos 2u - \frac{23e^2}{24} \right), \quad (13)$$

$$\dot{L} = \frac{32c^2 m \nu^2 x^{7/2} \sqrt{1 - e^2}}{5(1 - e \cos u)^5} \left(1 - \frac{1}{2}e \cos u - \frac{5e^2}{8} + \frac{1}{8}e^2 \cos 2u \right). \quad (14)$$

The instantaneous helical flux for the eccentric binary is

$$F_\xi = \frac{32c^5 \nu^2 x^5}{5G(1 - e \cos u)^6} \left\{ 1 - \frac{23e^2}{24} - \frac{e^2 \cos 2u}{24} - \sqrt{1 - e^2} (1 - e \cos u) \left(1 - \frac{1}{2}e \cos u - \frac{5e^2}{8} + \frac{1}{8}e^2 \cos 2u \right) \right\}, \quad (15a)$$

$$= \frac{48c^5 \nu^2 x^5 e \cos u}{5G} + \mathcal{O}(e^2). \quad (15b)$$

We present the orbit averaged expression for this flux as well. The expression matches with the averaged helical flux

derived in [19] for eccentric orbits

$$\langle F_\xi \rangle = \frac{32}{5G} c^5 \nu^2 x^5 \left\{ \frac{1}{(1-e^2)^{7/2}} \left(1 + \frac{73}{24} e^2 + \frac{37}{96} e^4 \right) - \frac{1}{(1-e^2)^2} \left(1 + \frac{7}{8} e^2 \right) \right\}, \quad (16a)$$

$$= \frac{352c^5\nu^2x^5e^2}{15G} + \mathcal{O}(e^2). \quad (16b)$$

The instantaneous and the averaged flux are non-linear in eccentricity and start at relative 0PN order with respect to the energy flux, as expected. In the limit of small eccentricity, they yield a simpler dependence on eccentricity.

B. Quasi-circular, non-precessing

Recent works have pushed PN results to 4.5PN order beyond the leading quadrupole radiation [3, 20]. This limits our helical flux calculation to 4.5PN accuracy.

To peek beyond the 4.5PN order, we estimate the leading order contribution to the helical flux from the source's l^{th} mass or current multipole moment. This approach gives a general understanding of the contribution to the helical flux from each multipole moment. We compare this prediction with the helical flux computed using numerical relativity simulations of binary black hole mergers.

1. Post-Newtonian helical flux

The helical flux requires the computation of energy and angular momentum flux as shown in Eq. (5). The energy flux has been computed in the literature up to 4.5PN order. This computation begins with constructing the metric perturbation in a Bondi-type coordinate system (u, \mathbf{X}) ,

$$h_{ab}^{\text{TT}} = \frac{4G}{c^2 R} \perp_{abij}(\mathbf{N}) \sum_{\ell \geq 2} \frac{1}{c^\ell \ell!} \left[N_{L-2} U_{ijL-2}(u) \right. \\ \left. - \frac{2\ell}{c(\ell+1)} N_{kL-2} \epsilon_{kl(i} V_{j)lL-2}(u) \right] + \mathcal{O}\left(\frac{1}{R^2}\right)$$

where $N^i = X^i/R$ and \perp_{abij} is the projection tensor. The metric perturbation is expressed in terms of radiative mass-type U_L and current-type V_L multipole moments in a transverse-traceless gauge. It is straightforward to obtain the multipole expansion of the energy flux using

Eq. (2),

$$\dot{E} = \sum_{l=2}^{\infty} \frac{G}{c^{2l+1}} \left[a_l U_L^{(1)} U_L^{(1)} + \frac{b_l}{c^2} V_L^{(1)} V_L^{(1)} \right], \quad (18)$$

where a_l and b_l are derived in [21], and the superscript numbers in parentheses denote retarded time derivatives, $U_L^{(j)} \equiv \frac{d^j}{du^j} U_L$. We account for the non-linear effects in gravitational wave propagation by relating the radiative multipole moments to the source (I_L, J_L) that describe the PN source. We achieve this using the intermediate canonical multipole moments (M_L, S_L) . The relation between radiative and canonical multipole moments contain instantaneous and hereditary type of terms up to a given PN order. Many of these relations have been derived in references [6, 20, 22–28]. At the stage of deriving the PN series for source multipole moments (I_L, J_L) , the procedure is specialized from generic orbits to quasi-circular orbits in the center-of-mass frame. Then we use the equations of motion for particles moving on these orbits for the computation of fluxes. As shown in [5], this procedure can be used to compute any Poincaré flux.

The recent 4.5PN-accurate expression for \dot{E} appears in Eq. (6.11) of [3], which they call \mathcal{F} . Here, we reproduce this existing computation and perform a similar computation for the angular momentum flux. The angular momentum flux can be expressed in terms of the radiative multipole moments U_L and V_L as

$$\dot{L}_i = \epsilon_{iab} \sum_{l=2}^{\infty} \frac{G}{c^{2l+1}} \left[a'_l U_{aL-1} U_{bL-1}^{(1)} + \frac{b'_l}{c^2} V_{aL-1} V_{bL-1}^{(1)} \right], \quad (19)$$

where the coefficients a'_l and b'_l are given in [5]. The 4.5PN-accurate expression for \dot{L} has not appeared in the literature, as far as we are aware, though it was *expected* to agree with \dot{E}/Ω . We have explicitly computed \dot{L} , accurate to 4.5PN order, using the equations of motion and the series expansions for U_L and V_L presented in [3, 5], using the xAct/xTensor suite for Mathematica [29, 30]. The magnitude of the angular momentum flux is

$$\begin{aligned}
\dot{L} = & \frac{32}{5} c^2 m \nu^2 x^{7/2} \left\{ 1 + \left[-\frac{1247}{336} - \frac{35}{12} \nu \right] x + 4\pi x^{3/2} + \left[-\frac{44711}{9072} + \frac{9271}{504} \nu + \frac{65}{18} \nu^2 \right] x^2 + \left[-\frac{8191}{672} - \frac{583}{24} \nu \right] \pi x^{5/2} \right. \\
& + \left[\frac{6643739519}{69854400} + \frac{16}{3} \pi^2 - \frac{1712}{105} \gamma_E - \frac{856}{105} \ln(16x) + \left(-\frac{134543}{7776} + \frac{41}{48} \pi^2 \right) \nu - \frac{94403}{3024} \nu^2 - \frac{775}{324} \nu^3 \right] x^3 \\
& + \left[-\frac{16285}{504} + \frac{214745}{1728} \nu + \frac{193385}{3024} \nu^2 \right] \pi x^{7/2} + \left[-\frac{323105549467}{3178375200} + \frac{232597}{4410} \gamma_E - \frac{1369}{126} \pi^2 + \frac{39931}{294} \ln 2 - \frac{47385}{1568} \ln 3 + \frac{232597}{8820} \ln x \right. \\
& + \left(-\frac{1452202403629}{1466942400} + \frac{41478}{245} \gamma_E - \frac{267127}{4608} \pi^2 + \frac{479062}{2205} \ln 2 + \frac{47385}{392} \ln 3 + \frac{20739}{245} \ln x \right) \nu + \left(\frac{1607125}{6804} - \frac{3157}{384} \pi^2 \right) \nu^2 \\
& + \left. \frac{6875}{504} \nu^3 + \frac{5}{6} \nu^4 \right] x^4 + \left[\frac{265978667519}{745113600} - \frac{6848}{105} \gamma_E - \frac{3424}{105} \ln(16x) + \left(\frac{2062241}{22176} + \frac{41}{12} \pi^2 \right) \nu - \frac{133112905}{290304} \nu^2 - \frac{3719141}{38016} \nu^3 \right] \pi x^{9/2} \\
& + \mathcal{O}(x^5) \left. \right\}. \tag{20}
\end{aligned}$$

We outline the procedure to compute the hereditary integrals involved in this computation in the appendix. Using these flux expressions, we compute the helical flux as expressed in Eq. (5).

$$F_\xi = 0 + \mathcal{O}(x^{10}). \tag{21}$$

This verifies the expectation that the helical flux vanishes up to 4.5PN order. In the next subsection, we calculate that the first non-vanishing PN order of the helical flux is at a relative 5PN order.

2. Abstract computation of helical flux

Given the limitations of the post-Newtonian results, we perform a non-rigorous computation to estimate the PN order for the leading order term in helical flux relative to energy flux. Similar to Eq. (19), the helical flux can be expressed in terms of the radiative multipole moments through a simple computation

$$\begin{aligned}
F_\xi = & \sum_{l=2}^{\infty} \frac{G}{c^{2l+1}} \left\{ a_l \left(\mathbf{U}_L^{(1)} \mathbf{U}_L^{(1)} - \Omega^i \epsilon_{iab} l U_{aL-1} \mathbf{U}_{bL-1}^{(1)} \right) \right. \\
& + \left. \frac{b_l}{c^2} \left(\mathbf{V}_L^{(1)} \mathbf{V}_L^{(1)} - \Omega^i \epsilon_{iab} l V_{aL-1} \mathbf{V}_{bL-1}^{(1)} \right) \right\}. \tag{22}
\end{aligned}$$

The estimate for the leading order term would require the Newtonian order relations between the radiative multipole moments and the source multipole moments that are given by

$$\mathbf{U}_L = \mathbf{I}_L^{(l)} + \mathcal{O}\left(\frac{1}{c^3}\right), \tag{23}$$

$$\mathbf{V}_L = \mathbf{J}_L^{(l)} + \mathcal{O}\left(\frac{1}{c^3}\right). \tag{24}$$

For circular, non-spinning binaries these source multipole moments can be related to orbital parameters of the binary to leading order as

$$\mathbf{I}_L = \mu \sigma_l(\nu) x_L + \mathcal{O}\left(\frac{1}{c}\right), \tag{25a}$$

$$\mathbf{J}_{L-1} = \mu \sigma_l(\nu) \epsilon_{ab\langle i_{l-1} x_{L-2} \rangle a} v_b + \mathcal{O}\left(\frac{1}{c}\right), \tag{25b}$$

where μ is the reduced mass and $\sigma_l(\nu)$ is a constant defined in [5]. The computation needs the equations of motion of the inspiralling circular binary system written in the form

$$x_i = r n_i, \tag{26a}$$

$$v_i = \epsilon_i^{jk} \Omega_j x_k + \frac{\dot{r}}{r} x_i, \tag{26b}$$

where x_i and v_i are the radius and velocity vectors of the reduced mass. For this calculation, we will refrain from explicitly substituting the equations of motion until the end, leaving derivatives in the form $x_i^{(k_i)}$. Using the generalized Leibniz rule, the l^{th} mass multipole moment can be expanded at leading order as

$$\mathbf{I}_L^{(l)} = \mu \sigma_l(\nu) \sum_{k_1 + \dots + k_l = l} \binom{l}{k_1, k_2, \dots, k_l} x_{i_1}^{(k_1)} x_{i_2}^{(k_2)} \dots x_{i_l}^{(k_l)}. \tag{27}$$

Since the flux is linear in the multipole moments, we can focus on the contribution from the l^{th} mass multipole moment to understand the general behavior,

$$\mathcal{F}_\xi(U_L) = U_{i_1 L-1}^{(1)} \left(U_{i_1 L-1}^{(1)} - \Omega^i \epsilon_{i j i_1} l U_{j L-1} \right) = I_{i_1 L-1}^{(l+1)} \left(I_{i_1 L-1}^{(l+1)} - \Omega^i \epsilon_{i j i_1} l I_{j L-1}^{(l)} \right), \quad (28)$$

$$= \mu^2 \sigma_l^2 \sum_{\Sigma m_i=l} \sum_{\Sigma k_i=l} \binom{l}{m_1, \dots, m_l} \binom{l}{k_1, \dots, k_l} l^2 x_{i_1}^{(m_1+1)} \left(x_{i_1}^{(k_1+1)} - \Omega^i \epsilon_{i j i_1} x_j^{(k_1)} \right) x_{i_2}^{(m_2)} x_{i_2}^{(k_2)} \dots x_{i_l}^{(m_l)} x_{i_l}^{(k_l)}, \quad (29)$$

where we substitute the radiative multipole moment with the source multipole moment in the second line. Using the quasicircular equations of motion in Eq. (26), it can be shown that

$$x_{i_1}^{(k_1+1)} = \epsilon_{i_1}{}^{jk} \Omega_j x_k^{(k_1)} + \left(1 - \frac{3}{2} k_1 \right) \left(\frac{\dot{r}}{r} \right) x_{i_1}^{(k_1)} + \mathcal{O} \left(\Omega x^{(k_1)} \frac{\dot{r}^2}{r^2 \Omega^2} \right) = \epsilon_{i_1}{}^{jk} \Omega_j x_k^{(k_1)} \left[1 + \mathcal{O} \left(\frac{\dot{r}}{r \Omega} \right) \right]. \quad (30)$$

The leading term of the above result (at 0PN relative order) cancels with the second term in Eq. (29). This leads to a manifest cancellation by 2.5PN orders, but there is also a subsequent cancellation by another 2.5PN orders:

$$\begin{aligned} \mathcal{F}_\xi(U_L) &= \mu^2 \sigma_l^2 \sum_{\Sigma m_i=l} \sum_{\Sigma k_i=l} \binom{l}{m_1, \dots, m_l} \binom{l}{k_1, \dots, k_l} \left(\frac{\dot{r}}{r} \right) \left(1 - \frac{3}{2} k_1 \right) l^2 x_{i_1}^{(m_1+1)} x_{i_1}^{(k_1)} \dots x_{i_l}^{(m_l)} x_{i_l}^{(k_l)} \left[1 + \mathcal{O} \left(\frac{\dot{r}}{r \Omega} \right) \right] \\ &= 0 + \mathcal{O} \left(\dot{E}(U_L) x^5 \right). \end{aligned} \quad (31)$$

The further cancellation by 2.5PN orders is due to the properties of a circular orbit. The 2.5PN order terms have $(2l+1)$ derivatives distributed over $(2l)$ separation vectors x_i , which are contracted together into several scalar terms. For a circular orbit in a plane, a term of the form $x_{i_j}^{(m_j)} x_{i_j}^{(k_j)}$ with an odd difference in derivatives leads to a contraction between perpendicular vectors in the plane. Therefore the only types of contractions that survive at the leading order are of the form $x_{i_j}^{(m_j)} x_{i_j}^{(k_j)}$ where the derivatives differ by an even integer, $m_j \equiv k_j \pmod{2}$. However, with $(2l+1)$ derivatives spread over $(2l)$ vectors, there will always be at least one term with an odd difference. Thus the first correction will be trivially zero and the first non-zero correction to the helical flux will appear at $\mathcal{O}(\dot{r}/r)^2$, that is a relative 5PN order to the energy flux contribution from the radiative multipoles U_L or V_L . We can see this computation for the quadrupole moment as

$$\mathcal{F}_\xi(U_{ij}) = \frac{212992c^5}{875G} \nu^4 x^{10} + \mathcal{O}(x^{21/2}). \quad (32)$$

Thus the contribution to the helical flux from the quadrupole moment is at a relative 5PN order from its contribution to the energy flux. Though this method is not rigorous, it agrees with our numerical results below.

IV. NUMERICAL RESULTS

We take ideas from existing analytical results to obtain comparable predictions of the PN order of the helical flux from numerical simulations. In the PN formalism [5], the frequency related parameter x is used to express the analytical results for fluxes and other relevant quantities.

The helical flux would have a similar series in x given by

$$F_\xi = a_0 x^p (1 + a_1 x + a_2 x^2 + \dots), \quad (33)$$

where a_i and p are as yet unknown. The numerical relativity waveforms from quasi-circular binaries give an advantage when estimating such unknown power law behavior. Since the effect is anticipated at a high PN order, the leading power can be obtained through an instantaneous PN order computation

$$\begin{aligned} \text{PN Order} &= p \approx \frac{d \log F_\xi}{d \log x}, \\ p &\approx \frac{3}{2} \times \frac{d \log F_\xi}{d \log \Omega}. \end{aligned} \quad (34)$$

We use 113 quasi-circular ($e < 10^{-4}$) non-precessing $\chi_{i\perp} < 10^{-4}$) NR simulations from the SXS catalog [11] to perform this analysis. Numerically, we compute the flux and angular velocity using the `scri` python package [31, 32]. We compare this numerical estimate of the instantaneous PN order with the prediction from the analytical results presented in the previous section. This numerical analysis runs into some subtleties.

The first obstacle arises from a lack of understanding of a unique definition of angular velocity to be obtained from numerical waveforms. In this work, we choose to work with two definitions of angular velocity: one that tries to maintain the strain to be a constant in a co-rotating frame [32], and another obtained from the phase of the h_{22} mode. We compare the results of these two approaches below.

The second set of issues is associated with the numerical attributes of the gravitational waveforms. The high degree of cancellation in the helical flux is due to the circular nature of the orbit. However, the numerical waveforms aren't produced from perfectly circular simulations. The

helical flux is modulated by the presence of eccentricity. We handle these modulations by smoothing the flux with a Gaussian kernel. The next subsections present the mathematical details of the choice of angular velocity and the smoothing process.

1. Angular velocity by minimal rotation

A commonly-used definition for quasi-circular binaries was proposed by Boyle in [32], inspired by earlier work [33]. Boyle's proposal is based on finding an instantaneous rotation to keep a waveform as constant as possible in a corotating frame, by minimizing

$$\Xi(\vec{\Omega}) = \int_{S^2} |i \vec{\Omega} \cdot \vec{L} f + \partial_t f|^2 d^2S, \quad (35)$$

where the \vec{L} differential operator is the infinitesimal generator of rotations, $L_a = -i\epsilon_{ab}{}^c x^b \partial_c$. Here the waveform $f(u, \theta, \phi)$ can be e.g. the GW strain or the news. The optimal $\vec{\Omega}$ is found as

$$\vec{\Omega}_{\text{rot}}(u) = -\langle \vec{L} \vec{L} \rangle^{-1} \cdot \langle \vec{L} \partial_t \rangle, \quad (36)$$

where the vector and matrix here have components

$$\langle \vec{L} \partial_t \rangle^a \equiv \sum_{\ell, m, m'} \text{Im} \left[\bar{f}_{(\ell, m')} \langle \ell, m' | L^a | \ell, m \rangle f_{(\ell, m)} \right], \quad (37a)$$

$$\langle \vec{L} \vec{L} \rangle^{ab} \equiv \sum_{\ell, m, m'} \bar{f}_{(\ell, m')} \langle \ell, m' | L^a L^b | \ell, m \rangle f_{(\ell, m)}. \quad (37b)$$

The structure of Eq. (35) resembles to the action of the helical Killing vector on the waveform. Therefore the numerical definition of $\vec{\Omega}_{\text{rot}}$ is attempting to enforce the helically symmetric condition on the waveform modes. Therefore it is rather circular to use this $\vec{\Omega}_{\text{rot}}$ to analyze how well the helical symmetry is satisfied. Nonetheless, we perform this analysis, which agrees with the second choice of angular velocity.

2. Angular velocity from (2, 2) mode phase

The dominant (2, 2) mode can be decomposed into an amplitude A_{22} and phase ϕ_{22} , which can be used to obtain the angular velocity via

$$h_{22} = A_{22}(t) e^{i\phi_{22}(t)}, \quad (38a)$$

$$\Omega_{22} = \left| \frac{1}{2} \frac{d\phi_{22}(t)}{dt} \right|. \quad (38b)$$

We compare these different choices below.

3. Results

These definitions can be used to compute the angular velocity numerically. We presented the helical fluxes from

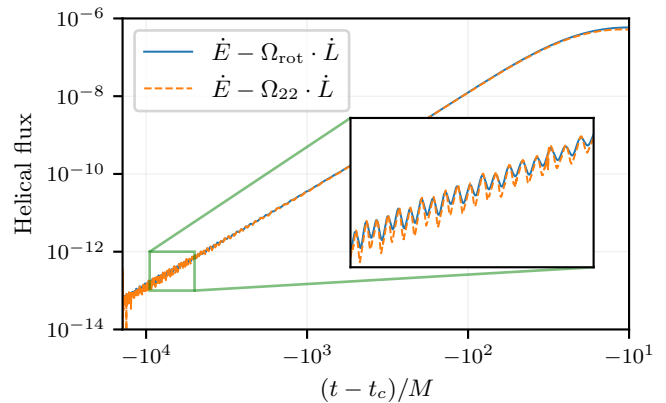


FIG. 3. Oscillations in the helical flux computed for a quasi-circular non-precessing binary (SXS:BBH:1154) with $e = 5.68 \times 10^{-5}$. Both angular velocity definitions— Ω_{rot} (blue) and Ω_{22} (orange)—exhibit modulations in the helical flux.

an eccentric, a precessing, and a non-precessing quasi-circular system in Fig. 2, demonstrating the cancellations at different PN orders for the three systems. Now we focus just on quasi-circular systems, which have the highest degree of cancellation.

In Fig. 3, we present the helical flux computed using the two definitions of angular velocity. The modulations present in helical flux are on the orbital timescales for both curves. This suggests that the oscillations are due to the small eccentricity ($e < 10^{-4}$, for our case) of the binary. For a perfectly quasi-circular binary, this flux would be smooth. Therefore we have to filter out or remove these orbital oscillations to disentangle the effect of eccentricity. This is achieved by performing moving averages on orbital timescales of the required quantities. The moving average is numerically performed by convolving the function with an appropriate kernel that filters out the high-frequency oscillations in the time domain. We use a normalized Gaussian kernel centered at a given t_i with variance given by the orbital timescale near t_i . The Gaussian kernel is

$$G(t - t_i) = \frac{1}{N} \exp\left(-\frac{1}{2} \frac{(t - t_i)^2}{\sigma_i^2}\right), \quad (39)$$

where $N = \sum_j G(t_j - t_i) \Delta t_j$ is the normalization factor and $\Delta t_j = t_j - t_{j-1}$. The moving average is represented by $\langle \cdot \rangle$ and performed numerically as

$$\begin{aligned} \langle f_i \rangle &= \sum_j G(t_j - t_i) f_j \Delta t_j, \\ &= \sum_j \frac{1}{N} \exp\left(-\frac{1}{2} \frac{(t_j - t_i)^2}{\sigma_i^2}\right) f_j \Delta t_j, \end{aligned} \quad (40)$$

where $\sigma_i = (2\pi/\Omega(t_i))$. We implement the following numerical procedure to get a prediction of the instantaneous PN order from each waveform:

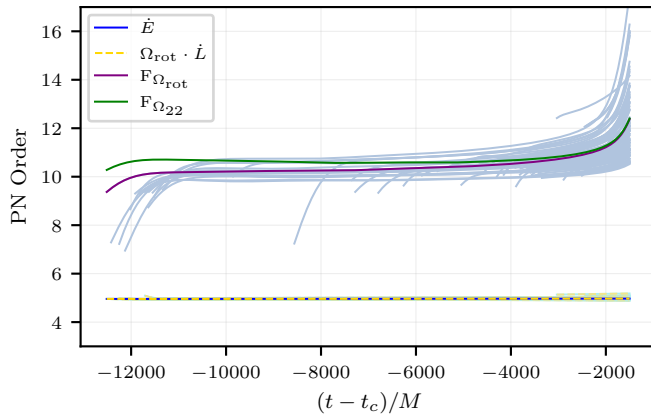


FIG. 4. The instantaneous PN order computed for 113 SXS simulations. The curves in the foreground are for a quasi-circular non-precessing simulation, SXS:BBH:1154. The helical flux is computed using both Ω_{rot} (purple) and $\Omega_{(2,2)}$ (green). For reference, the yellow and blue curves correspond to the instantaneous PN orders of \dot{E} and $\Omega \cdot \dot{L}$ respectively.

1. Obtain the longest segment of time when $|\Omega|$ is monotonically increasing.
2. Compute the helical flux F_ξ using Eq. (5) in this monotonically increasing segment.
3. Perform a moving average to smooth the modulations in F_ξ .
4. Construct a cubic spline of $\log \langle F_\xi \rangle$ as a function of $\log \Omega$.
5. Compute the instantaneous PN order using spline derivatives.
6. Average out the oscillations in the instantaneous PN order computation to get a smooth curve via

$$\text{Smoothed PN Order} = \frac{3}{2} \times \left\langle \frac{d \log \langle F \rangle}{d \log \Omega} \right\rangle. \quad (41)$$

All the resultant quantities are computed in the longest monotonic segment of $|\Omega|$. Eccentricity can make either Ω_{rot} or Ω_{22} be oscillatory, limiting the range of times when we can construct the spline. We plot the smoothed PN order in Fig. 4. We find that the instantaneous PN order of the helical flux is at 5PN order relative to the energy flux. We can clearly see that both angular velocities give comparable predictions of the instantaneous PN order. These numerical results support the analytical calculation presented in Sec. III B 2 thus establishing that the effect of radiation reaction breaks the symmetry at such a high PN order.

V. DISCUSSION AND CONCLUSIONS

In this work we investigated the approximate helical symmetry observed in compact binary systems. The effects of eccentricity, precession, and radiation reaction push a binary system away from being helically symmetric. We quantify the breaking of this symmetry by computing the flux of the charge corresponding to the symmetry. Each of these effects can be studied using numerical waveforms by systematically controlling the initial orbital parameters of the binary.

For quasi-circular non-precessing binary systems, we analytically predicted that the dominant contribution to the helical flux comes from the quadrupole moment. The PN order of the helical flux starts at a 5PN order relative to its contribution to the energy flux. The analytical prediction agrees with our numerical computation of the instantaneous PN order of the helical flux. A robust analytical comparison requires PN results that are not yet available in the literature. We leave the computation of this exact analytical expression of helical flux for future work.

In the numerical analysis, we realized a subtlety in the choice of angular velocity (Ω) used to compute the helical flux. We used two definitions of Ω : Ω_{rot} minimizes the waveform's time dependence in a corotating frame, and Ω_{22} is obtained from the phase of the dominant (2, 2) mode of the strain. The subtlety here is that Ω_{rot} effectively tries to impose a helical symmetry, thus making the calculation of helical flux somewhat circular. Nonetheless, these two choices give comparable computations of the instantaneous PN order.

We have been wary of the oscillations observed in the helical flux for quasi-circular non-precessing binary. The initial data for these simulations are not perfectly quasi-circular, thus small initial eccentricities produce modulations in the helical flux. Therefore, we chose to filter out these modulations by performing Gaussian convolution.

For eccentric non-precessing binary systems, we analytically computed the instantaneous helical flux. As expected, the helical flux is non-vanishing at the leading 0PN order relative to the energy flux. In the limit of small eccentricity, the helical flux has a linear relation to eccentricity. It would be interesting to compare this relation using numerical waveforms. However, we will need a different definition of angular velocity for eccentric systems. This comparison is left for future work.

For precessing binary systems, we expect moderate cancellation in the helical flux. As observed in Fig. 2, precession is the second largest effect breaking the helical symmetry. A robust analytical computation is required for obtaining the helical flux with PN results to sufficiently high order. The numerical analysis runs into similar subtleties as in the case of quasi-circular non-precessing binaries. We will need a well-justified numerical splitting between orbital angular velocity and precession angular velocity, which agrees with the post-Newtonian prediction of precession. For both precession and eccentricity, we

will need a more careful averaging procedure to avoid filtering out real physical modulations. A careful analysis of these effects is left for future work.

ACKNOWLEDGMENTS

We would like to thank Aaron Zimmerman, Katerina Chatziioannou, Davide Gerosa, David Trestini, Éanna Flanagan, Alexandre Le Tiec, and Harald Pfeiffer for valuable discussions and feedback on this work. This work

was supported by NSF CAREER Award PHY–2047382 and a Sloan Foundation Research Fellowship.

Appendix A: Computation of memory intergral

The flux computation involves hereditary integrals arising from both tail and non-linear interactions. For example, the dominant tail starts at 1.5PN order and the non-linear interaction first appears at 2.5PN order. These integrals for the $l = 2$ moment take the form

$$U_{ij}^{1.5\text{PN}} = \frac{2GM}{c^3} \int_0^\infty d\tau M_{ij}^{(4)}(u-\tau) \left[\ln\left(\frac{c\tau}{2b_0}\right) + \frac{11}{12} \right], \quad (\text{A1})$$

$$U_{ij}^{2.5\text{PN}} = \frac{G}{c^5} \left\{ -\frac{2}{7} \int_0^\infty d\tau \left[M_{a(i}^{(3)} M_{j)a}^{(3)} \right] (u-\tau) + \frac{1}{7} M_{a(i}^{(5)} M_{j)a} - \frac{5}{7} M_{a(i}^{(4)} M_{j)a}^{(1)} - \frac{2}{7} M_{a(i}^{(3)} M_{j)a}^{(2)} + \frac{1}{3} \epsilon_{ab(i} M_{j)a}^{(4)} S_b \right\}, \quad (\text{A2})$$

where M_{ij} and S_i are the canonical mass and spin multipole moments, respectively, and b_0 is an arbitrary constant that cancels out at the end of the flux calculation. We follow the procedure outlined in [3, 5, 8] to compute these integrals. By expanding canonical multipole moments using the PN series derived in [6, 20, 22, 27, 28], we obtain the hereditary integrals in terms of the source and gauge multipole moments. The latest PN results for source and gauge multipole moments in terms of binary's parameters have been provided in [23–26]. At this stage we incorporate the quasircular behavior of binary's orbit and use the equations of motion to compute derivatives. For the case of quasircular orbits, an adiabatic approximation has been used in earlier work to compute the integrals up to 3.5PN precision. This approximation assumes that the radius (r) and orbital frequency (Ω) of the binary remain constant during integration. However, this approximation breaks for the dominant tail, Eq. (A1), that is needed up to 2.5PN precision for the 4PN flux computation. The higher order hereditary terms, like Eq. (A2), can still be handled using the adiabatic approximation.

As shown in [8], the hereditary integrals involve many

scalar products between the orbital vectors x^i or v^i , evaluated at the current time u or at earlier time $(u-\tau)$. The products we need to perform the integrals are

$$x^i x'_i = r r' \cos(\phi - \phi'), \quad (\text{A3a})$$

$$x^i v'_i = r r' \Omega' \sin(\phi - \phi') + r \dot{r}' \cos(\phi - \phi'), \quad (\text{A3b})$$

$$v^i x'_i = -r' r \Omega \sin(\phi - \phi') + r' \dot{r} \cos(\phi - \phi'), \quad (\text{A3c})$$

$$v^i v'_i = r \Omega r' \Omega' \cos(\phi - \phi') + \dot{r} r' \Omega' \sin(\phi - \phi') - r \Omega \dot{r}' \sin(\phi - \phi') + \mathcal{O}(x^5). \quad (\text{A3d})$$

Here unprimed and primed quantities refer to the state of the binary at two different times, e.g. at u and at $u-\tau$. For the integrals that require post-adiabatic corrections, we incorporate time (or τ) dependence on r' and Ω' . By converting these variables involved in terms of the parameter $y = \left(\frac{Gm\Omega}{c^3}\right)^{2/3}$, these expressions reduce to the type of integrals presented in Section 3.4.2 of [5]. Thus we use standard formulas to compute these hereditary integrals and truncate the result to the required PN order. These contributions are combined with the instantaneous terms to obtain the total flux.

-
- [1] E. Gourgoulhon, P. Grandclement and S. Bonazzola, *Binary black holes in circular orbits. 1. A Global space-time approach*, *Phys. Rev. D* **65** (2002) 044020 [[gr-qc/0106015](#)].
- [2] P. Grandclement, E. Gourgoulhon and S. Bonazzola, *Binary black holes in circular orbits. 2. Numerical methods and first results*, *Phys. Rev. D* **65** (2002) 044021 [[gr-qc/0106016](#)].
- [3] L. Blanchet, G. Faye, Q. Henry, F. Larrouturou and D. Trestini, *Gravitational-wave flux and quadrupole modes from quasircular nonspinning compact binaries to the fourth post-Newtonian order*, *Phys. Rev. D* **108** (2023) 064041 [[2304.11186](#)].
- [4] L. Bernard, L. Blanchet, G. Faye and T. Marchand, *Center-of-Mass Equations of Motion and Conserved Integrals of Compact Binary Systems at the Fourth Post-Newtonian Order*, *Phys. Rev. D* **97** (2018) 044037 [[1711.00283](#)].
- [5] L. Blanchet, *Post-Newtonian theory for gravitational waves*, *Living Rev. Rel.* **27** (2024) 4.
- [6] G. Faye, S. Marsat, L. Blanchet and B.R. Iyer, *The third and a half post-Newtonian gravitational wave quadrupole mode for quasi-circular inspiralling compact binaries*, *Class. Quant. Grav.* **29** (2012) 175004 [[1204.1043](#)].

- [7] K.G. Arun, L. Blanchet, B.R. Iyer and M.S.S. Qusailah, *Tail effects in the 3PN gravitational wave energy flux of compact binaries in quasi-elliptical orbits*, *Phys. Rev. D* **77** (2008) 064034 [0711.0250].
- [8] L. Blanchet, *Energy losses by gravitational radiation in inspiraling compact binaries to five halves postNewtonian order*, *Phys. Rev. D* **54** (1996) 1417 [gr-qc/9603048].
- [9] A. Le Tiec, L. Blanchet and B.F. Whiting, *The First Law of Binary Black Hole Mechanics in General Relativity and Post-Newtonian Theory*, *Phys. Rev. D* **85** (2012) 064039 [1111.5378].
- [10] P. Ramond and A. Le Tiec, *First law of mechanics for spinning compact binaries: Dipolar order*, *Phys. Rev. D* **106** (2022) 044057 [2202.09345].
- [11] M. Boyle et al., *The SXS Collaboration catalog of binary black hole simulations*, *Class. Quant. Grav.* **36** (2019) 195006 [1904.04831].
- [12] E. Noether, *Invariant Variation Problems*, *Gott. Nachr.* **1918** (1918) 235 [physics/0503066].
- [13] T. Apostolatos, D. Kennefick, E. Poisson and A. Ori, *Gravitational radiation from a particle in circular orbit around a black hole. 3: Stability of circular orbits under radiation reaction*, *Phys. Rev. D* **47** (1993) 5376.
- [14] H. Bondi, M.G.J. van der Burg and A.W.K. Metzner, *Gravitational waves in general relativity. 7. Waves from axisymmetric isolated systems*, *Proc. Roy. Soc. Lond. A* **269** (1962) 21.
- [15] R. Sachs, *Asymptotic symmetries in gravitational theory*, *Phys. Rev.* **128** (1962) 2851.
- [16] R.K. Sachs, *Gravitational waves in general relativity. 8. Waves in asymptotically flat space-times*, *Proc. Roy. Soc. Lond. A* **270** (1962) 103.
- [17] E.E. Flanagan and D.A. Nichols, *Conserved charges of the extended Bondi-Metzner-Sachs algebra*, *Phys. Rev. D* **95** (2017) 044002 [1510.03386].
- [18] N. Loutrel and N. Yunes, *Hereditary Effects in Eccentric Compact Binary Inspirals to Third Post-Newtonian Order*, *Class. Quant. Grav.* **34** (2017) 044003 [1607.05409].
- [19] A. Le Tiec, *First Law of Mechanics for Compact Binaries on Eccentric Orbits*, *Phys. Rev. D* **92** (2015) 084021 [1506.05648].
- [20] T. Marchand, L. Blanchet and G. Faye, *Gravitational-wave tail effects to quartic non-linear order*, *Class. Quant. Grav.* **33** (2016) 244003 [1607.07601].
- [21] K.S. Thorne, *Multipole Expansions of Gravitational Radiation*, *Rev. Mod. Phys.* **52** (1980) 299.
- [22] G. Faye, L. Blanchet and B.R. Iyer, *Non-linear multipole interactions and gravitational-wave octupole modes for inspiralling compact binaries to third-and-a-half post-Newtonian order*, *Class. Quant. Grav.* **32** (2015) 045016 [1409.3546].
- [23] T. Marchand, Q. Henry, F. Larroutou, S. Marsat, G. Faye and L. Blanchet, *The mass quadrupole moment of compact binary systems at the fourth post-Newtonian order*, *Class. Quant. Grav.* **37** (2020) 215006 [2003.13672].
- [24] F. Larroutou, Q. Henry, L. Blanchet and G. Faye, *The quadrupole moment of compact binaries to the fourth post-Newtonian order: I. Non-locality in time and infra-red divergencies*, *Class. Quant. Grav.* **39** (2022) 115007 [2110.02240].
- [25] F. Larroutou, L. Blanchet, Q. Henry and G. Faye, *The quadrupole moment of compact binaries to the fourth post-Newtonian order: II. Dimensional regularization and renormalization*, *Class. Quant. Grav.* **39** (2022) 115008 [2110.02243].
- [26] Q. Henry, G. Faye and L. Blanchet, *The current-type quadrupole moment and gravitational-wave mode $(\ell, m) = (2, 1)$ of compact binary systems at the third post-Newtonian order*, *Class. Quant. Grav.* **38** (2021) 185004 [2105.10876].
- [27] L. Blanchet, G. Faye and F. Larroutou, *The quadrupole moment of compact binaries to the fourth post-Newtonian order: from source to canonical moment*, *Class. Quant. Grav.* **39** (2022) 195003 [2204.11293].
- [28] D. Trestini, F. Larroutou and L. Blanchet, *The quadrupole moment of compact binaries to the fourth post-Newtonian order: relating the harmonic and radiative metrics*, *Class. Quant. Grav.* **40** (2023) 055006 [2209.02719].
- [29] “xAct: Efficient tensor computer algebra for the Wolfram Language.” <http://www.xact.es/>.
- [30] J.M. Martín-García, *xPerm: fast index canonicalization for tensor computer algebra*, *Comp. Phys. Commun.* **179** (2008) 597 [0803.0862].
- [31] M. Boyle, D. Iozzo, L. Stein, A. Khairnar, H. Rüter, M. Scheel et al., *scri*, June, 2024. 10.5281/zenodo.12585016.
- [32] M. Boyle, *Angular velocity of gravitational radiation from precessing binaries and the corotating frame*, *Phys. Rev. D* **87** (2013) 104006 [1302.2919].
- [33] R. O’Shaughnessy, B. Vaishnav, J. Healy, Z. Meeks and D. Shoemaker, *Efficient asymptotic frame selection for binary black hole spacetimes using asymptotic radiation*, *Phys. Rev. D* **84** (2011) 124002 [1109.5224].